

Assessing Guest Diffusivities in Porous Hosts from Transient Concentration Profiles

Lars Heinke,¹ Despina Tzoulaki,¹ Christian Chmelik,¹ Florian Hibbe,¹ Jasper M. van Baten,² Hyuna Lim,³ Jing Li,³ Rajamani Krishna,² and Jörg Kärger¹

¹*Faculty of Physics and Geosciences, Department of Interface Physics, University of Leipzig, Linnéstrasse 5, 04103 Leipzig, Germany*

²*Van't Hoff Institute for Molecular Sciences, University of Amsterdam, Nieuwe Achtergracht 166, 1018 WV Amsterdam, The Netherlands*

³*Department of Chemistry and Chemical Biology, Rutgers University, 610 Taylor Road, Piscataway, New Jersey 08854, USA*

(Received 22 September 2008; published 11 February 2009)

Using the short-chain-length alkanes from ethane to *n*-butane as guest molecules, transient concentration profiles during uptake or release (via interference microscopy) and tracer exchange (via IR microimaging) in Zn(tbip), a particularly stable representative of a novel family of nanoporous materials (the metal organic frameworks), were recorded. Analyzing the spatiotemporal dependence of the profiles provides immediate access to the transport diffusivities and self-diffusivities, yielding a data basis of unprecedented reliability for mass transfer in nanoporous materials. As a particular feature of the system, self- and transport diffusivities may be combined to estimate the rate of mutual passages of the guest molecules in the chains of pore segments, thus quantifying departure from a genuine single-file system.

DOI: 10.1103/PhysRevLett.102.065901

PACS numbers: 66.30.je, 66.30.Pa, 68.43.Jk

Owing to most recent significant developments in material sciences [1] and driven by the fascinating prospects of technical application [2], the diversity of nanoporous materials is continuously increasing [3]. Diffusion is among those processes which may decide about the technological performance of these materials [4–6]. Simultaneously, it is one of the most fundamental phenomena and the investigation of diffusion under confinement [7,8] is among the hot topics of current fundamental research. Thus, diffusion in nanoporous materials is addressed in numerous publications, with many of them developing theoretical concepts for the explanation of experimental data [9–12]. However, beginning with the application of the pulsed field gradient nuclear magnetic resonance to diffusion studies with zeolites [5,13,14], the experimental determination of reliable diffusivities in nanoporous host-guest systems proved to be far from trivial. In fact, in numerous cases “real” specimens of nanoporous material turned out to notably deviate from the ideal textbook structure, with the possibility that these deviations (pore blockage, cracks), rather than diffusion in the genuine pore space, become rate determining for the observed transport phenomena [15,16]. This constraint is of immediate impact on molecular modeling, since it is the experimental evidence which has to serve as the ultimate criterion of its validity.

Among the numerous techniques applied to diffusion measurement in nanoporous materials [5,6,14,17], only the recently introduced methods of interference microscopy [16,18–20] and IR microimaging [16] [supplementary material (SM) 1 and 2 [21]] are able to monitor transient concentration profiles and, hence, diffusion fluxes directly in the interior of individual nanoporous crystallites. To our knowledge, never before in any type of matter could diffusion-driven transient concentration profiles be ob-

served with a similar wealth of information [22,23]. Moreover, by following tracer exchange, IR microimaging is also able to operate under (quasi-) equilibrium conditions. The virtue of these techniques, namely, to focus on a particular, isolated crystal, raises the problem that the number of adsorption or desorption cycles which could be performed with an individual crystal remained rather limited due to sample instabilities. Though to different extents, for most of the investigated specimens the transport parameters were eventually found to change with increasing cycle numbers. With the advent of Zn(tbip) (H_2 tbip = 5-*tert*-butyl isophthalic acid) [24], a highly stable representative of the family of microporous metal organic frameworks (MOFs), we dispose of a nanoporous host system for which an essentially unlimited reproducibility in subsequent adsorption-desorption cycles could be observed. Zn(tbip) (see Fig. 1 and SM 4) is traversed by an array of parallel chains of pore segments in the direction of longitudinal crystal extension. The resulting one-dimensionality of diffusion and structural stability make MOFs of type Zn(tbip) excellent candidates for a systematic, experimentally founded investigation of the key features of mass transfer in nanoporous materials.

Altogether, more than 60 different adsorption and desorption runs with three different guest molecules (ethane, propane, and *n*-butane) and three runs of tracer exchange (between propane and deuterated propane at two different loadings) have been performed. All measurements were carried out at room temperature (298 K). The adsorption and desorption experiments were initiated by a stepwise variation of the pressure in the surrounding gas atmosphere which can be assumed to occur essentially instantaneously. For observing tracer exchange, after equilibration with the host system, the molecules in the surrounding atmosphere were replaced by their isotopes. Examples of the evolution

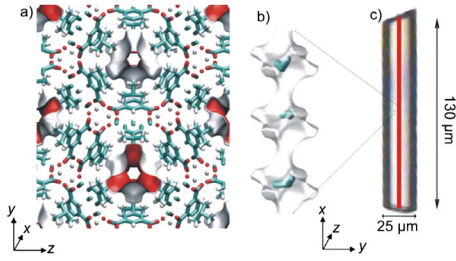


FIG. 1 (color online). Model representation (a),(b) and image (c) of the MOF Zn(tbip) under study. The atoms of the crystal framework and the one-dimensional pore structure. The side pockets are ordered like two three-leafed clover separated by windows of a diameter of 0.45 nm. The red (or gray) surface indicates the surface of the pores as perceived by the guest molecules. (c) Crystal under investigation. The red (or gray) line indicates that the profiles are recorded in the center of the crystal.

of the thus recorded concentration profiles are shown in Figs. 2 and 3, as well as in the SM 1 and 2. It is worthwhile mentioning that, following recent studies with notably poorer spatiotemporal resolution [25,26], it is only the introduction of IR microimaging by focal-plane array detection [27] that allowed the observation of the transient tracer exchange profiles of the quality shown in Fig. 2.

In all experiments, the boundary concentration does not immediately reach the equilibrium value. This indicates an additional transport resistance at the surface, i.e., a reduced surface permeability [28]. Reference to the underlying transport parameters has to take account, therefore, of both the intracrystalline diffusivities and surface permeabilities. Intracrystalline diffusivities are defined as factors of proportionality between particle fluxes and concentration gradients, surface permeabilities as factors of proportionality between particle fluxes and the difference between the actual boundary concentration and the concentration in equilibrium with the surrounding atmosphere [4,5,13,14] (see also SM 5). If observed under overall concentration gradients, they are referred to as “transport”

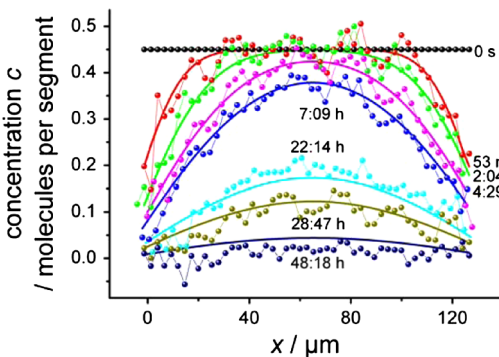


FIG. 2 (color online). Transient concentration profiles of deuterated propane in MOF Zn(tbip) during tracer exchange with the undeuterated isotope at an overall pressure of 60 mbar. Thin lines represent the best fits of the analytical expressions for tracer exchange with a constant surface permeability and diffusivity.

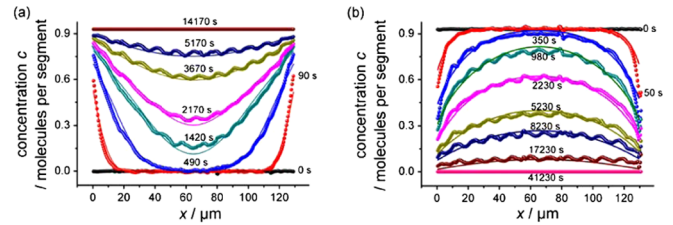


FIG. 3 (color online). Transient concentration profiles of propane in Zn(tbip) during adsorption [0 to 480 mbar (a)] and desorption [480 mbar to vacuum (b)]. The thin lines represent the best fits of the numerical solution with a concentration dependence of the surface permeability and the diffusivity provided by a Reed-Ehrlich ansatz.

diffusivities (permeabilities), if observed by tracer exchange, they are self- (or tracer exchange) diffusivities (permeabilities). The experimental accessible space scale exceeds the nanoscale (pore distance) of the material by several orders of magnitude so that the relevant relations of mass transfer end up in a continuous diffusion equation (Fick’s 1st and 2nd laws, SM 5).

During tracer exchange, profile evolution is therefore controlled by a single value of the (tracer or self-) diffusivity and surface permeability (depending on the overall concentration), rather than on the (varying) concentration of labeled (or unlabeled) molecules. Figures 4(b) and 4(e) show the data which yield best fits between the measured curves and their theoretical prediction (full lines in Fig. 2, as well as in Fig. S4 [21]) by the standard relations of

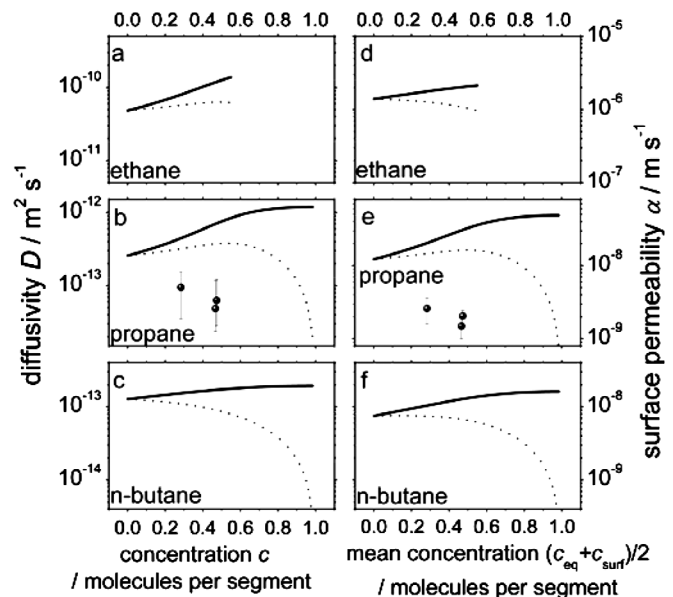


FIG. 4. Diffusivity (left) and surface permeability (right) of ethane, propane, and *n*-butane in Zn(tbip) as resulting as a best fit to the experimentally determined transient concentration profiles. The results from (nonequilibrium) uptake or release experiments are presented by full lines, the tracer exchange data by points. The corrected (MS) parameters used in the fitting procedure are indicated by dotted lines.

molecular uptake or release with constant diffusivities and surface permeabilities [5,29] (SM 6).

Under transient uptake and release, account has to be taken of a possible concentration dependence of both the intracrystalline (transport) diffusivity and the surface permeability. By means of the adsorption isotherm $c(p)$ (SM 3), the transport diffusivity can be related to a ‘‘Maxwell-Stefan’’ (MS, or ‘‘corrected’’) diffusivity D_0 by the relation [4,5,9]

$$D_T = \frac{\partial \ln p}{\partial \ln c} D_0. \quad (1)$$

The equilibrium concentrations $c(p)$ of propane and n -butane are found to follow a single-site-Langmuir isotherm with a maximum loading of one molecule per (channel) segment, while Configurational-Bias Monte Carlo (CBMC) simulations show that ethane occupies two different adsorption sites (SM 3,4).

By considering only nearest-neighbor interaction on a surface of equal adsorption sites, Reed and Ehrlich derived the following analytical expression of the concentration dependence of diffusion [30–32]:

$$D_0 = D_0(0) \frac{(1 + \varepsilon)^{z-1}}{(1 + \varepsilon/\phi)^z}, \quad (2)$$

with

$$\varepsilon = \frac{(\beta - 1 + 2\theta)\phi}{2 - 2\theta}, \quad (3)$$

$$\beta = \sqrt{1 - 4\theta(1 - \theta)(1 - 1/\phi)}. \quad (4)$$

z is the coordination number (number of nearest neighbors), which equals 2 for one-dimensional systems. θ denotes the occupancy, i.e., the concentration divided by the maximum concentration, c/c_{\max} . Most remarkably (and conveniently), over the total range of concentrations the diffusivity is found to be determined by only two parameters, namely, the MS diffusivity $D_0(0)$ at zero loading (coinciding with the transport and self-diffusivity at this loading) and the ‘‘interaction’’ parameter ϕ (>1 for repulsive and <1 for attractive interaction, see SM 5). In the limiting case of simple hard-core interaction ($\phi = 1$), Eq. (2) simplifies to the lattice-gas relation $D_0 \sim (1 - \theta)$ [33,34]. In many studies the observed concentration dependencies were found to nicely follow an analytical expression provided by Eqs. (1)–(4) [12,32]. Using this ansatz for both the diffusivities and surface permeabilities,

we attained an excellent reproduction of the transient concentration profiles also in our experiments. This is visualized by the full lines in the representations of the transient concentration profiles. They have been calculated with the diffusivities and surface permeabilities with the concentration dependences resulting by inserting the fitting parameters summarized in Table I into Eqs. (2) to (4) by a numerical solution of the diffusion equation [29,35]. Most importantly, this agreement is demonstrated to exist for both adsorption and desorption, confirming reproducibility and reversibility of the measurements. Figure 4 summarizes the concentration dependences of the transport diffusivities and surface permeabilities determined in our studies. As well included are the corresponding ‘‘corrected’’ quantities resulting from the respective adsorption isotherms via Eq. (1).

The simultaneous measurement of transport diffusion and self-diffusion allows an assessment of up to which extent mass transfer in the chain of pore segments in Zn(tbip) is subject to single-file diffusion [36–39]. In a perfect single-file system of N sites (pore segments) the effective self-diffusivity of tracer exchange is known to be exceeded by $D_0(0)$ by a factor of $N\theta/(1 - \theta)$ [40–42]. With crystal lengths $\geq 100 \mu\text{m}$ and a site distance of $\lambda \approx 1 \text{ nm}$, the resulting factors dramatically exceed the experimental values [Fig. 4(b)] of about 2 and 5 for $\theta = 0.28$ and 0.48, respectively. Hence, within the chains of pore segments in the crystals under study the propane molecules must definitely have the possibility of mutual passages. The passage rate Γ of a particular pair of adjacent molecules is related to the tracer (or self-) diffusivity D^* by the simple random-walk expression

$$D^* = l^2 \Gamma \quad (5)$$

where $l(\approx \lambda/\theta)$ denotes the mean distance between adjacent molecules. With the simplifying assumption that a jump attempt towards an empty segment is always successful, while it is only successful with the probability p if this segment is occupied, the passage rate may be correlated by the expression

$$\Gamma = \frac{p(1 - \theta)}{2\tau} \quad (6)$$

with the mean time τ between jump attempts. Inserting Eq. (6) into (5) yields

$$D^* = \frac{\lambda^1}{2\tau} \frac{p(1 - \theta)}{\theta^2} = D_0(0) \frac{p(1 - \theta)}{\theta^2}, \quad (7)$$

TABLE I. Reed-Ehrlich parameters used for the construction of the concentration dependencies of the transport diffusivities and surface permeabilities following Eqs. (1)–(4), yielding best fits to the recorded concentration profiles.

Guest molecule	$D_0(0)$	ϕ_D	$\alpha_0(0)$	ϕ_α	Standard deviation between measured and recalculated concentrations profiles
Ethane	$5.2 \times 10^{-11} \text{ m}^2 \text{ s}^{-1}$	2.6	$1.3 \times 10^{-6} \text{ m s}^{-1}$	2.1	4.4%
Propane	$2.4 \times 10^{-13} \text{ m}^2 \text{ s}^{-1}$	4.9	$2.7 \times 10^{-8} \text{ m s}^{-1}$	2.9	3.8%
n -butane	$1.3 \times 10^{-13} \text{ m}^2 \text{ s}^{-1}$	1.5	$7.6 \times 10^{-9} \text{ m s}^{-1}$	2.1	3.1%

from which one obtains passage probabilities of $p = 5.5 \times 10^{-2}$ and 8.8×10^{-2} for $\theta = 0.28$ and 0.48 , respectively. The increase of p with increasing loading may be referred to the repulsive interaction of the diffusants which, in the chosen model approach, has already been found to give rise to values >1 for the fitting parameter ϕ of concentration dependence.

On applying the concentration dependence of the Reed-Ehrlich model, we have made use of a most versatile option of representing a large spectrum of possible concentration dependences by a minimum of free parameters. The measured concentration profiles are in excellent agreement with the corresponding solutions of the diffusion equation with the thus described diffusivities and permeabilities (Table I). However, with the successful application of the concentration dependence as following from the Reed-Ehrlich model, the model can clearly not automatically be assumed to adequately represent the microdynamic features of mass transfer. The substantial data spectrum covering three different chain lengths and a large range of concentrations is rather expected to give rise to the application of more refined techniques of molecular modeling and to their comparison with experimental evidence.

Financial support by Deutsche Forschungsgemeinschaft (R.K., International Research Group "Diffusion in Zeolites" and International Research Training Group "Diffusion in Porous Materials"), Max-Buchner-Forschungsförderung, INDENS Marie-Curie program, and Studienstiftung des Deutschen Volkes are gratefully acknowledged.

-
- [1] B. Wang *et al.*, *Nature (London)* **453**, 207 (2008).
 [2] M. Eddaoudi *et al.*, *Science* **295**, 469 (2002).
 [3] S. Kitagawa, R. Kitaura, and S. Noro, *Angew. Chem., Int. Ed.* **43**, 2334 (2004).
 [4] R. Krishna and J. M. van Baten, *Chem. Eng. Sci.* **63**, 3120 (2008).
 [5] J. Kärger and D. M. Ruthven, *Diffusion in Zeolites and Other Microporous Solids* (Wiley & Sons, New York, 1992).
 [6] N. Y. Chen, T. F. Degnan, and C. M. Smith, *Molecular Transport and Reaction in Zeolites* (Wiley-VCH, New York, 1994).
 [7] Q. H. Wei, C. Bechinger, and P. Leiderer, *Science* **287**, 625 (2000).
 [8] L. A. Clark, G. T. Ye, and R. Q. Snurr, *Phys. Rev. Lett.* **84**, 2893 (2000).
 [9] H. Jobic and D. Theodorou, *Microporous Mesoporous Mater.* **102**, 21 (2007).
 [10] E. Beerdsen, D. Dubbeldam, and B. Smit, *Phys. Rev. Lett.* **96**, 044501 (2006).
 [11] R. Haberlandt, S. Fritzsche, and H. L. Vörtler, in *Handbook of Surfaces and Interfaces of Materials*, edited by H. S. Nalwa (Academic Press, New York, 2001), Vol. 5, p. 357.
 [12] R. Krishna and J. M. v. Baten, *Microporous Mesoporous Mater.* **109**, 91 (2008).
 [13] J. Kärger, *Leipzig, Einstein, Diffusion* (Leipziger Universitätsverlag, Leipzig, 2007).
 [14] D. M. Ruthven and M. F. M. Post, in *Introduction to Zeolite Science and Practice*, edited by H. van Bekkum, E. M. Flanigen, P. A. Jacobs, and J. C. Jansen (Elsevier, Amsterdam, 2001), p. 525.
 [15] C. Chmelik, P. Kortunov, S. Vasenkov, and J. Kärger, *Adsorption* **11**, 455 (2005).
 [16] L. Heinke *et al.*, *Chem. Eng. Technol.* **30**, 995 (2007).
 [17] H. Jobic, J. Kärger, and M. Bee, *Phys. Rev. Lett.* **82**, 4260 (1999).
 [18] J. Kärger *et al.*, *Angew. Chem., Int. Ed.* **45**, 7846 (2006).
 [19] U. Schemmert *et al.*, *Europhys. Lett.* **46**, 204 (1999).
 [20] D. Tzoulaki *et al.*, *Angew. Chem., Int. Ed.* **47**, 3954 (2008).
 [21] See EPAPS Document No. E-PRLTAO-102-059907 for supplementary material on infrared microimaging, recorded concentration profiles, adsorption isotherms, Monte Carlo simulations, mass transfer in nanoporous materials, and the Reed-Ehrlich model. For more information on EPAPS, see <http://www.aip.org/pubservs/epaps.html>.
 [22] W. Jost, *Diffusion in Solids, Liquids and Gases* (Academic Press, New York, 1960).
 [23] P. Heitjans and J. Kärger, *Diffusion in Condensed Matter: Methods, Materials, Models* (Springer, Berlin, Heidelberg, 2005).
 [24] L. Pan *et al.*, *J. Am. Chem. Soc.* **128**, 4180 (2006).
 [25] D. R. Kodali, D. M. Small, J. Powell, and K. Krishnan, *Appl. Spectrosc.* **45**, 1310 (1991).
 [26] E. Lehmann *et al.*, *J. Am. Chem. Soc.* **124**, 8690 (2002).
 [27] Y. Roggo, A. Edmond, P. Chalus, and M. Ulmschneider, *Anal. Chim. Acta* **535**, 79 (2005).
 [28] L. Heinke, P. Kortunov, D. Tzoulaki, and J. Kärger, *Phys. Rev. Lett.* **99**, 228301 (2007).
 [29] J. Crank, *The Mathematics of Diffusion* (Clarendon Press, Oxford, 1975).
 [30] D. A. Reed and G. Ehrlich, *Surf. Sci.* **102**, 588 (1981).
 [31] R. Krishna, D. Paschek, and R. Baur, *Microporous Mesoporous Mater.* **76**, 233 (2004).
 [32] G. K. Papadopoulos, H. Jobic, and D. N. Theodorou, *J. Phys. Chem. B* **108**, 12748 (2004).
 [33] P. Kortunov *et al.*, *J. Am. Chem. Soc.* **129**, 8041 (2007).
 [34] K. W. Kehr, K. Mussawisade, G. M. Schütz, and T. Wichmann, in *Diffusion in Condensed Matter-Methods, Materials, Models*, edited by P. Heitjans and J. Kärger (Springer, Berlin, 2005), p. 975.
 [35] L. Heinke and J. Kärger, *New J. Phys.* **10**, 023035 (2008).
 [36] K. Hahn, J. Kärger, and V. Kukla, *Phys. Rev. Lett.* **76**, 2762 (1996).
 [37] C. Lutz, M. Kollmann, and C. Bechinger, *Phys. Rev. Lett.* **93**, 026001 (2004).
 [38] M. Kollmann, *Phys. Rev. Lett.* **90**, 180602 (2003).
 [39] F. Marchesoni and A. Taloni, *Chaos* **17**, 043112 (2007).
 [40] S. Vasenkov and J. Kärger, *Phys. Rev. E* **66**, 052601 (2002).
 [41] C. Rödenbeck and J. Kärger, *J. Chem. Phys.* **110**, 3970 (1999).
 [42] P. H. Nelson and S. M. Auerbach, *J. Chem. Phys.* **110**, 9235 (1999).